Notice

This manuscript is a non-peer reviewed preprint that has been submitted to EarthArXiv. Please be aware that newer versions of this document may exhibit minor differences, including slight content variations.

Manuscript Details

Title: WaterGate: An Accessible Computational Model of Flooding Patterns
Authors: Navvye Anand, George Cheng, Tyler Rose
Contact Email: navvyeanand@gmail.com

WATERGATE: AN ACCESSIBLE COMPUTATIONAL MODEL OF FLOODING PATTERNS

Navvye Anand
Sanskriti School
New Delhi, Delhi, India
navvyeanand@gmail.com

George Cheng
North Carolina School of Science and Math
Durham, North Carolina, United States
gcheng713@gmail.com

Tyler Rose
Wolfram Research
Cupertino, California, United States
tylerr@wolfram.com

ABSTRACT

240 million people are affected by floods each year, reflecting the urgent need for accessible flood prediction and detection. WaterGate is a computational model that uses geographic elevation data and the rational method to predict flooding patterns , generating an interactive 3D model for user accessibility. Computational hydrology applies numerical methods, machine learning algorithms, and computational simulations to understand, predict, and manage water resources --- including floods. Our project employs computational hydrology by analyzing the structure of river tributaries in 2D through polygon clustering, satellite imaging, and various cleaning protocols. We developed respective tributary tree graphs, morphological graphs, and nodes to create a comprehensive tree and 3D model. Afterward, we examine the morphology of flood plains in 3D space, implementing the rational method ($Q = CiA$) framework with curated relief plots to predict, model, and visualize flooding elevation. Then, we constructed our stream order analysis, waterline delineation, and statistical analysis to validate our date. Lastly, we modeled different river systems and developed further extensions to increase the applicability of WaterGate to communities around the world.

Keywords computational hydrology · flooding patterns · rational model · Wolfram language

1 Introduction

1.1 Progression of Severe Floods

Every year, an estimated 240 million individuals confront the unsettling realities of flooding [1]. The severity and frequency of these devastating events have spiraled upward in the past few decades, largely fueled by the interplay of several factors such as climate change, rapid urbanization, deforestation, and misguided land management strategies [2]. Historically, floods were often viewed as localized, rare events. However, in the face of rapid global change, the narrative has shifted drastically [3]. An increasing body of evidence indicates an uptick in high-intensity floods in many regions across the globe [4]. Climate change, marked by a consistent rise in global temperatures, has intensified the hydrologic cycle, resulting in greater evaporation rates, increased atmospheric water vapor, and consequently, more extreme rainfall events [3]. This sequence of changes fuels the occurrence of more severe floods. For instance, the cyclone-induced floods in Mozambique, Zimbabwe, and Malawi resulted in over 1,000 fatalities, rendered millions homeless, and inflicted widespread infrastructural damage [5].

The relentless march of urbanization, when poorly planned and managed, has further aggravated flooding incidents [6]. By replacing permeable natural surfaces with impervious materials like asphalt and concrete, urbanization

enhances runoff during rainfall, escalating flood risks. The 2011 Bangkok floods in Thailand exemplify this phenomenon; over 800 lives were lost, with more than 13 million people affected [7]. Unregulated urban expansion in the capital city amplified the flood magnitude, underlining the implications of uncontrolled urban development on flood severity. Historically significant floods, like the Great Mississippi Flood of 1927, underscore the critical need for comprehensive flood management strategies [8]. This event is remembered not just for its vast physical destruction, but also for its far-reaching socioeconomic and political implications. The lack of proper flood control mechanisms exacerbated the catastrophe, instigating policy changes in the US [8].

Yet, despite the lessons learned, itś apparent that current flood management systems require further refinement [9]. This escalating trend of severe flood events underlines the pressing need for improved, reliable, and accessible flood prediction technologies.

1.2   Installation

Computational hydrology is a field that harnesses the power of computer science to simulate and understand complex water systems, presenting a significant evolution in the analysis and prediction of hydrological phenomena [10]. Traditional hydrology depended largely on field observations and mathematical equations to describe water cycles but lacked the sophistication to handle the inherent complexity and variability of these systems [11]. The integration of numerical methods into hydrology in the mid-20th century marked a significant advancement, providing the capability to solve complex mathematical models that better represent physical systems [12]. The advent of the digital computer during the same period further propelled these developments, enabling researchers to process larger sets of data and solve more complex equations [13]. Yet, the true power of computational hydrology began to unfold with the integration of remote sensing data and Geographic Information Systems (GIS) in the late 20th century [14]. Remote sensing allowed hydrologists to monitor large-scale hydrological events in real-time, while GIS provided the tools to analyze, visualize, and model these events in their geographical context [15].

In recent years, machine learning has been increasingly adopted in computational hydrology. Machine learning algorithms, with their ability to identify complex patterns in large datasets, offer a promising avenue for improving the accuracy of hydrological models [16]. Yet, while these techniques are powerful, their "black box" nature often makes them difficult to interpret, raising important questions about their place in the field [10]. Today, computational hydrology stands at the forefront of hydrological research, providing indispensable tools for predicting and managing water resources, including floods. Projects like WaterGate reflect the latest efforts in this field, utilizing the power of computational hydrology to create accessible, user-friendly flood prediction models, providing invaluable tools for communities worldwide in the face of escalating flood events.

1.3   Application of the Wolfram Language

The Wolfram Language, a versatile universal computational language created by British scientist Stephen Wolfram, has found significant applications in the field of computational hydrology [17]. Its built-in capabilities for symbolic computation, data visualization, and advanced analytics are leveraged for solving complex water-related problems.

The Wolfram Language's adept data-handling capabilities make it an attractive choice for tasks such as data import/export, wrangling, cleaning, and preprocessing [18]. Its flexible and readable syntax allows efficient manipulation of large data sets, leading to improved productivity in data-driven hydrological analyses. The language's built-in capabilities for symbolic and numerical computations make it useful for implementing mathematical models used in hydrology. From simpler concepts such as the Rational Method to complex differential equation-based models, the Wolfram Language's computational capabilities allow for clear implementation and testing of these models [19].

Data visualization is an essential part of computational hydrology, aiding in the interpretation of results and communication of findings. The Wolfram Language's robust plotting and graphical capabilities facilitate the generation of complex geospatial visuals, relief maps, contour plots, and 3D models for studying river dynamics, flood patterns, and water resources management [20]. Furthermore, the Wolfram Language's in-built machine learning capabilities offer opportunities for predictive modeling in hydrology. These tools can help hydrologists identify patterns in historical data, make predictions about future events like floods or droughts, and develop strategies for water management [18].

Overall, the Wolfram Language's multiparadigm approach, versatile coding paradigms, and high-level functionality position it as a robust tool for addressing diverse challenges in computational hydrology, enhancing understanding and management of water resources, and hence the use in WaterGate.

2 Methodology

2.1 Use of Satellite Imagery and Geographic Elevation

Satellite imagery and geographic elevation data provide an invaluable resource for a range of applications, from environmental studies to urban planning and flood prediction. The Wolfram Language, extensively used in Mathematica, provides powerful functionalities to process, analyze, and visualize this geospatial data, offering an advantageous platform for such applications [21]. The Wolfram Language has built-in functions to directly import and manipulate satellite imagery from various sources. "GeoImage" allows users to retrieve satellite images for specified geographic locations, and "ImageAdjust" and "Colorize" can be used to enhance these images for better visual interpretation [21]. "ImageCorrelate" can identify similarities in satellite images, useful in tracking changes in landscapes over time. These capabilities make the Wolfram Language a potent tool in satellite image analysis. Furthermore, Wolfram Language is equipped with comprehensive functionalities for handling geographic elevation data. "GeoElevationData" returns the elevation data for any specified region in various formats, facilitating detailed topographical analysis [21]. "GeoGraphics" provides powerful tools to visualize geographic and elevation data, allowing users to generate 2D and 3D models of landscapes, including river systems and floodplains. "GeoIdentify" can classify different geographic features, supporting the identification of river tributaries and potential flood zones.

In the context of WaterGate, for instance, these built-in functions are used to import and process satellite imagery and geographic elevation data, identify river tributaries, create interactive 3D models of floodplains, and apply machine learning algorithms to refine flood predictions.

2.2 Current Flood Prediction Systems

Flood prediction systems have evolved significantly over the years, leveraging advancements in technology and computational capabilities to predict hydrological events with increased accuracy and lead time. Several systems are currently in use worldwide, each with unique methodologies and strengths [22].

The most traditional systems are hydrological models, which are mathematical representations of the water cycle and associated processes [12]. These models can range from simple empirical models to complex physically-based simulations. While these models have improved over time, they often rely heavily on accurate weather predictions and can struggle with the inherent uncertainties of predicting rainfall patterns [10]. More advanced systems integrate GIS and Remote Sensing (RS) technologies. These systems utilize data from satellites, radars, and other remote sensing tools to gather real-time data about hydrological variables like rainfall, soil moisture, and river levels [11]. They then use GIS to model and visualize these variables geographically. These systems offer significant improvements in spatial and temporal resolution but can be complex and expensive to implement [15]. Ensemble prediction systems have also gained traction, integrating multiple models or methods to provide a range of possible outcomes. These systems account for the uncertainty inherent in flood prediction and provide a probabilistic outlook that can be extremely valuable for decision-makers [22].

Despite these advancements, predicting floods remains a challenging endeavor due to the complex and variable nature of hydrological systems. Continuous improvements in data collection, computational techniques, and modeling strategies are crucial to enhancing the accuracy and reliability of flood prediction systems.

2.3 Current Identification of River Tributaries

Traditionally, topographic maps have been used for identifying river tributaries. However, this approach is labor-intensive and subject to human error, especially in regions with complex river networks [14]. With the advent of remote sensing technology, satellite imagery and aerial photography have been employed to delineate river tributaries. Satellite-based remote sensing provides wide-area coverage and regular updates, making it particularly useful for tracking temporal changes in river systems [23]. However, cloud cover and vegetation can sometimes hinder the identification process. In addition to satellite imagery, digital elevation models (DEMs) have proven invaluable in river tributary identification. DEMs provide a 3D representation of the Earth's surface, facilitating the extraction of hydrological features such as river networks. Using algorithms like D8, D-Infinity, and Rho8, researchers can determine flow direction and accumulation to delineate watersheds and identify river tributaries [24]. Convolutional Neural Networks (CNNs), in particular, have shown great promise in image-based river detection tasks [25].

Despite the advances in tributary identification, challenges remain. These include difficulties in identifying small tributaries, differentiating rivers from other linear features, and detecting temporary or intermittent water channels.

Further research and technological advancements are needed to overcome these challenges and improve the accuracy and efficiency of river tributary identification.

2.4 The Rational Method

The Rational Method, represented by the formula $Q = CiA$, is a long-standing, time-tested approach used for calculating peak stormwater discharge – an important factor in flood analysis and urban drainage design. In this formula, Q is the peak discharge, C is the runoff coefficient, i is the rainfall intensity, and A is the drainage area [26]. Developed in the mid-19th century, the Rational Method's simplicity has contributed to its lasting popularity, despite the advent of more complex hydrological models. The method is particularly suited for small, urbanized watersheds where the response to rainfall events is relatively quick and consistent [15].

The runoff coefficient (C) represents the proportion of rainfall that transforms into the runoff, accounting for factors such as land use, soil type, and slope. Rainfall intensity (i) is typically obtained from Intensity-Duration-Frequency (IDF) curves specific to a particular geographic location. Drainage area (A) is often derived from topographic maps or DEMs [27].

However, the Rational Method has its limitations. It assumes a constant rainfall intensity throughout the storm event, which is rarely the case in nature. It's also less accurate for larger, rural watersheds with diverse topographies and land uses. Furthermore, it doesn't account for antecedent moisture conditions or temporal distribution of rainfall [26]. Despite these limitations, the Rational Method remains an essential tool in the toolkit of hydrologists and civil engineers. It serves as a first-order estimation of peak discharge and is widely used in preliminary design and planning due to its ease of application and simplicity [15]. Because the $Q = CiA$ framework is the most consistent measuring mechanism for water output in flash flood events, WaterGate will implement this framework as its core calculation equation.

2.5 WaterGate's Innovation

WaterGate's approach begins with the acquisition of comprehensive geographic elevation data, collected from various sources such as satellite imagery and DEMs. This robust dataset serves as the foundation for analysis, offering a detailed topographic representation of river systems and surrounding landscapes [24].

To identify river tributaries from this dataset, we apply a polygon clustering algorithm, a powerful computational technique that classifies and groups data points based on spatial relationships and morphological features [28]. We also incorporate machine learning algorithms to optimize this process, enabling WaterGate's system to learn and adapt to varying geographic and hydrological conditions. The use of machine learning equips WaterGate with the capacity to identify even small or temporary water channels, overcoming a significant challenge faced by conventional methods [25].

Once river tributaries are identified, we generate their respective tributary tree graphs. These graphs represent the hierarchical structure of the river system, which is essential for understanding how water flows through the network and how flooding events might unfold.

For floodplain creation, we turn to the $Q = CiA$ By integrating rainfall intensity data, runoff coefficients, and the area of the watershed, we can predict and model potential flooding scenarios [26]. Furthermore, using the identified river tributaries and their tree graphs, we simulate how water would disperse across the floodplain in the event of a flood. To facilitate better understanding and planning, we translate these predictions into interactive 3D models of the floodplains. We have also incorporated features for river basin graphage, basin overflow, and stream order for the sake of more accurately supplementing our original framework. Users can visually explore these models, gaining insight into potential flood patterns and assessing the risks associated with different flooding scenarios.

3 Results

3.1 Elevation Data in the Wolfram Language

The Wolfram Language has proven to be an extremely useful tool for visualizing elevation data. In particular, **GeoElevationData** can be used to view the elevation of a particular geo-location above sea-level. It can be manipulated to visualize elevation according to different paradigms. By default, it returns the orthometric height, which can be defined as the elevation above the surface of constant gravitational potential equal to that of mean sea level [17]. However, alternative heights, such as geodetic height and undulation height can be returned by

varying parameters. We primarily use the orthometric height functionality as it is the most reliable tool to measure height with respect to the mean sea level.

A relief map is a materialization of a terrain which is often used to facilitate the visual recognition of terrain features. In the Wolfram Language, the function **ReliefPlot** is used to generate a relief map (plot) from an array of height values, which can be obtained from **GeoElevationData**.
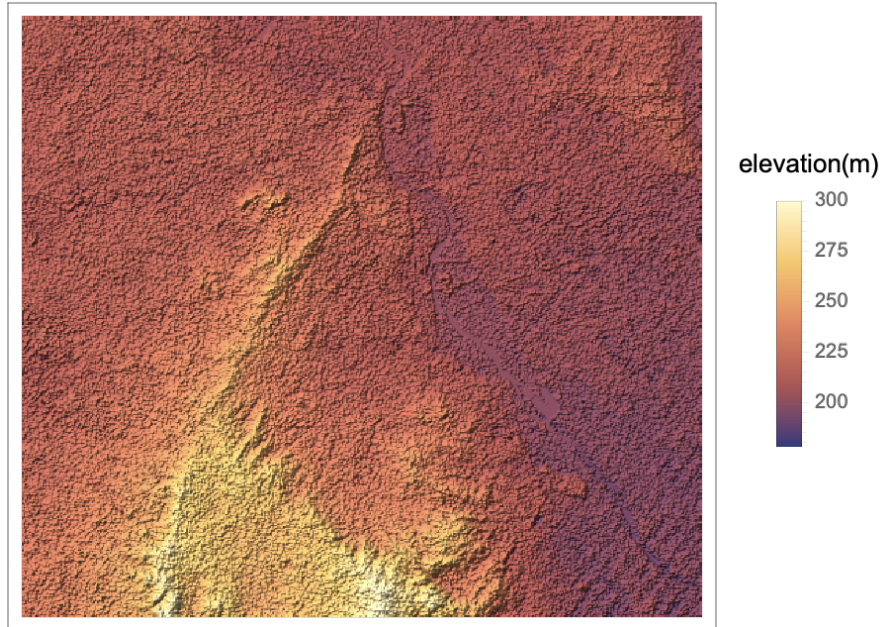

Figure 1 : Relief plot of New Delhi using GeoElevationData

3.2 Identification of Rivers and Tributaries in the Wolfram Language

Although the Wolfram Language is a computational powertool, current methods of analyzing river tributaries are limited to "notable" rivers and streams. This is due to the fact that rivers are not **GeoEntities** but rather only **Entities** in the Wolfram Language. Thus, river data extraction is extremely limited, and the database for "notable" rivers does not identify tributary points, connectedness, nor stream order identification. This section uses a novel approach to find rivers and tributaries in **GeoLocations** such as cities.We start by taking the example of Paris, and the river Marne, which acts as a tributary to the river Seine.
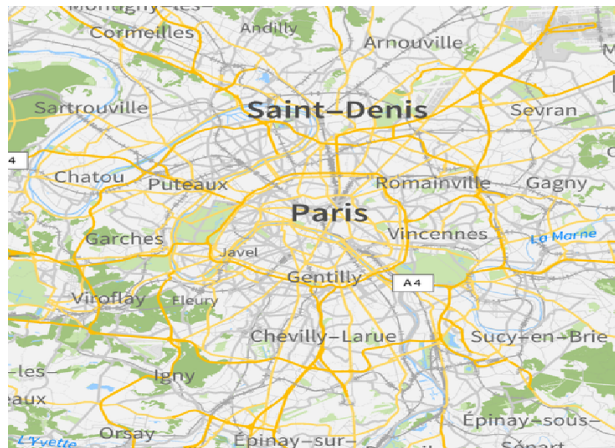

Figure 2 : Map of Paris using GeoLocations

Notice that the map appears to be a simplified version, and that is due to the **VectorMinimal** parameter which allows us to convert individual components on the map into manipulable polygons.

We can then visualize rivers by extracting water-related graphics from the above-mentioned map. This is done by identifying the water primitives by RGB-Color mapping.


Figure 3: Primitive river extraction using RGB-Color Map

However, there are still a few small-water bodies in this map which are not necessarily helpful to us. In order to remove said water bodies, we replace the small connected components with background pixels. In order to do this however, we need to first convert the above-mentioned image to a binary image, i.e, an image that consists of only black and white pixels. After converting, we can apply Otsu's algorithm to return a single intensity threshold that separates pixels into two classes, foreground and background. Those in the background will then get replaced by black pixels. All of this is done using the inbuilt function **DeleteSmallComponents**.

We can then adjust the image using **Thinning**, which is a mathematical operation similar to erosion that is used to reduce the width of an object's boundary to a single pixel. **Thinning** performs repeated iterations of erosion until it gets the desired result.The iterative process of thinning can be summarized as follows:

- Put the image through an erosion procedure. This entails scanning the entire image and determining the neighborhood of each foreground pixel.
- The pixel is kept if its neighborhood complies with a predetermined pattern; else, it is changed to background (black).
- Repeat the erosion process several times, until the image doesn't change any more.
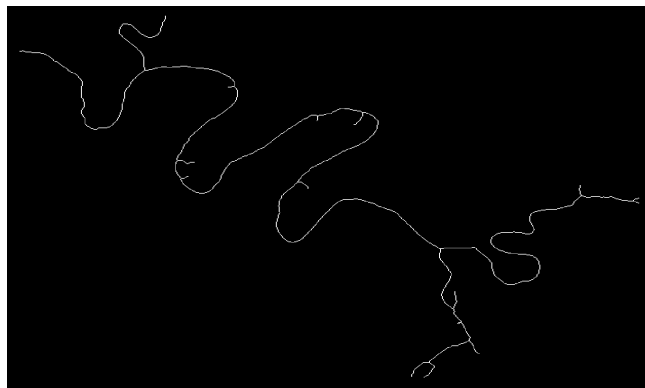

Figure 4: Marne River after cleaning

The **MorphologicalGraph** function uses mathematical morphology developed by Serra Et. al, 1986, to create a morphological graph on the basis of an image. The process of identifying morphological branch points and

endpoints in an image skeleton involves converting them into vertices. These vertices are then used to construct a graph, where each vertex represents a branch point or an endpoint. An undirected edge is created between two vertices if the corresponding branch points or endpoints are connected in an 8-connected manner within the skeleton.

There are a few properties in this **MorphologicalGraph** that are not suitable for river systems with large bodies of water. It cannot depict tributaries properly and cannot commensurate the distance between them. To overcome this limitation and make the morphological graph acyclic, we can employ the **TransitiveReductionGraph** function. Formally a transitive reduction of a graph G is another graph with the same vertices and as few edges as possible, such that for all pairs of vertices (V, W) a path from V to W in G exists iff such a path exists in the reduction. We use this functionality to convert the original morphological graph to an acyclic one, that is, a graph without any loops.
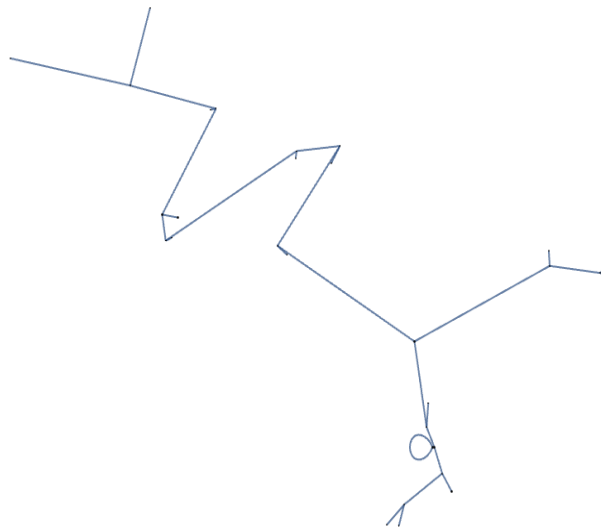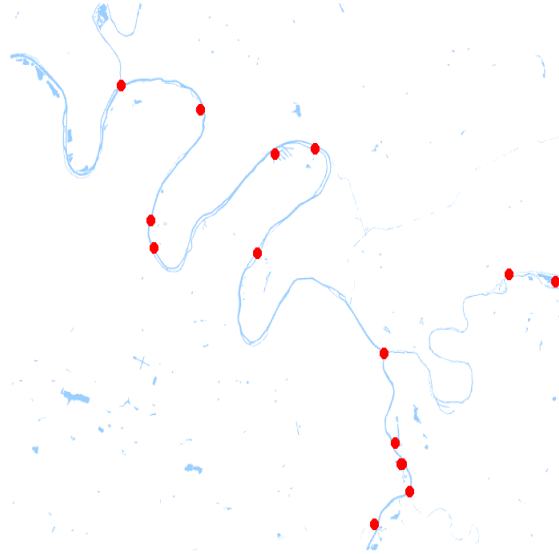

Figure 5: Morphological graph of the Marne

We can convert the acyclic morphological graph to a tree in order to gauge the structural information of the river, i.e, when it splits. And finally, we can apply **MorphologicalBranchPoints** to find the stream splits and apply various cleaning mechanisms to remove extraneous water sources and return the river to the original size.
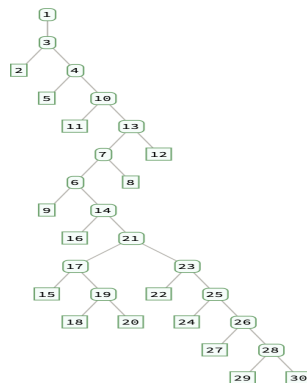
Figure 6 : Tree Graph of the Marne River.

Figure 7: Morphological BranchPoint graph of the MarneRiver.

### 3.3 Implementing Horton-Strahler Stream Order

The Horton-Strahler stream order is defined as a numerical measure of the branching complexity of a river. It was first developed by Robert E. Horton (1945) [29] and Arthur Newell Strahler (1952, 1957) [30, 31].

The process of assigning a Horton-Strahler number to a leaf in a tree is as follows :

- If the node is a leaf, then its Strahler number is one

- If the node has one child with Strahler number i, and all other children have Strahler numbers less than i, then the Strahler number of the node is i again.

- If the node has two or more children with Strahler number i, and no children with greater number, then the Strahler number of the node is $i + 1$

Implementing the Horton-Strahler algorithm in Mathematica is easy, and can be done by performing a Depth-First Search (DFS) followed by assigning the strahler-number after traversing the tree, essentially in postorder. A heuristic is shown below

- A variable represents the river network as an adjacency list, where each segment/node is associated with its downstream segments.

- strahlerNumbers is initialized with all segments having a Strahler number of 1.

- The DFS function is defined to traverse the river network using DFS, calculating Strahler numbers in a postorder manner.

- For each node, it calculates the Strahler number based on the Strahler numbers of its downstream segments.

- If all downstream segments have the same Strahler number, the node's Strahler number is incremented by 1.

- The process starts from root node(s) and traverses the network.
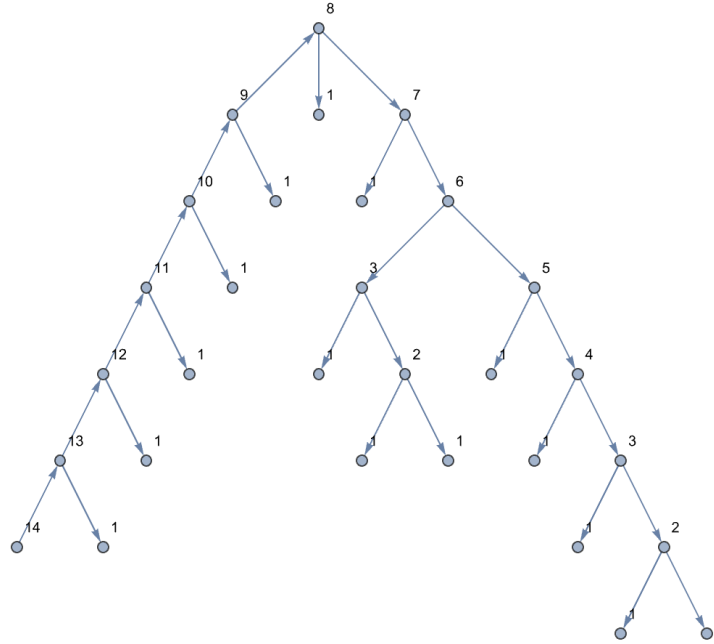
Figure 8: Implementation of the Horton-Strahler Number for the Marne

The Horton-Strahler algorithm has an accompanying ratio called the Bifurcation ratio. The nth Bifurcation Ratio can be defined as the the ratio of number of vertices of order i to the number of vertices of order $(i + 1)$

$$B_i = \frac{n_i}{n_{i+1}}$$

The overall bifurcation ratio is calculated by taking the average of all the bifurcation ratios of order i. In this case, it's **1.57692.**

3.4   Implementing the Rational Method

The rational method is used for determining peak discharges; this method is traditionally used to size storm sewers, channels, and other stormwater structures.The Rational Method expresses a relationship between rainfall intensity and catchment area as independent variables and the peak flood discharge resulting from the rainfall as the dependent variable.

The Rational method is appropriate for estimating peak discharges for small drainage areas of up to about 200 acres (80 hectares) with no significant flood storage. The method provides the designer with a peak discharge value, but does not provide a time series of flow nor flow volume. The rational method formula is expressed as $Q = CiA$ where:

- Q = Peak rate of runoff

- C= Runoff coefficient

- i = Average intensity of rainfall

- A = The Watershed Area

Using the Wolfram Language, we will be calculating each of these variables and parameterizing them for any geographic location.

RUNOFF COEFFICIENTS FOR THE RATIONAL FORMULA			
Typical Composite Runoff Coefficients by Land Use		Normal Range of Runoff Coefficients	
Area Description	C-value	Surface Characteristic	C-value
Business		**Lawns**	
Downtown Areas	0.70-0.95	Sandy Soil, Flat (2%)	0.05-0.10
Neighborhood Areas	0.50-0.70	Sandy Soil, Ave. (2-7%)	0.10-0.15
		Sandy Soil, Steep (>7%)	0.15-0.20
Residential		Heavy Soil, Flat (2%)	0.13-0.17
Single Family Areas	0.30-0.50	Heavy Soil, Ave. (2-7%)	0.18-0.22
Multi-Units (detached)	0.40-0.60	Heavy Soil, Steep (>7%)	0.2500.35
Multi-Units (attached)	0.60-0.75		
Suburban	0.25-0.40	**Agricultural**	
Apartments	0.50-0.70	Bare Packed Soil	
		Smooth	0.30-0.60
Industrial		Rough	0.20-0.50
Light Use	0.50-0.80	Cultivated Rows	
Heavy Use	0.60-0.90	Heavy Soil, no crop	0.30-0.60
Railroad Yards	0.20-0.35	Heavy Soil, with crop	0.20-0.50
Unimproved Areas	0.10-0.30	Sandy Soil, no crop	0.20-0.40
		Sandy Soil, with crop	0.10-0.25
Park		Pasture	
Park/Cemeteries	0.10-0.25	Heavy Soil	0.15-0.45
Playgrounds	0.20-0.35	Sandy Soil	0.05-0.25
Pavement		**Woodland**	0.05-0.25
Asphalt and Concrete	0.70-0.95		
Brick	0.70-0.85		
Roof	0.75-0.95		

The presented C-values are typical for return periods of 2-10-year storms with the higher values for the larger design storms. Judgement must be used to select the appropriate C-value within the range for the land use. Generally, larger areas with permeable soils, flat slopes, and dense vegetation should have the lower C-value; and smaller areas with low permeability soils, steep slopes and sparse vegetation should be assigned higher a C-value.

Figure 9: Table for $Q = CiA$

3.4.1 Calculations for implementing the Rational Method

Finding Runoff Coefficient

As colors from different regions may differ, we have to build an algorithm that converts the closest color to the colors in our key. Using **Nearest** and **ReplaceAll** we are able to associate the correct colors with the correct weights. Afterwards we can see the color coverage of all the regions in the map using "**Color**" and "**Coverage**" as the option for the**DominantColors** function - in which pixels are grouped into clusters of dominant colors using a standard k-means clustering algorithm. Finally, we substitute the color weights to get our runoff coefficient value.

Finding the intensity of the rainfall

Using previous literature, we found that the intensity of rainfall for flash floods is usually around 4-6 inches; by taking the rainfall data using **WeatherData** for the past 20+ years, we are able to find an average annual rainfall. We then map the intensity of rainfall (if it were to flood) and set it proportional to the annual rainfall.

Finding the Area

We can find the area of a city or a region by converting it to a polygon. We can then compute the area assuming that neighboring points of the polygon are joined by geodesic paths. Alternatively, we could also measure the local distortion of an area induced by a geo projection around a given location - comparing the global nominal scale to the local distortion area.

River Runoff Model

We calculate the **PeakRunoff** for the city of Juneau, Alaska to be 794982.0. In order to create a river runoff model - we want to multiply the **PeakRunoff** calculation Q by the inverse of rainwater flowing into the river basin to model the increase factor of the river by which the river will increase with respect to time.

As an example, we can use our newly found $Q = CiA$ river elevation increase to calculate a 1422.29 feet increase if it rained for 750 hours straight in Juneau, Alaska. We can also create both relief plots and flood plain graphs using this data.
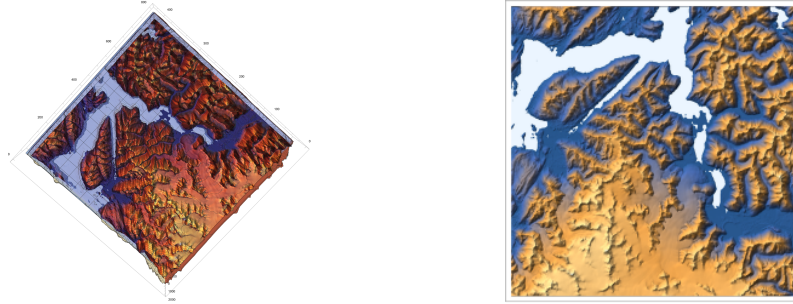
Figure 10: Relief plot and flood plain for Juneau, Alaska.

3.5 Watershed Delineation

Watershed delineation refers to the process of identifying the boundary of a water-basin, drainage basin or catchment. It is an extremely important process in the fields of environment science and hydrology.We start by taking the Magnitude of the elevation of Sundarbans National Park, a famous delta basin system in India and Bangladesh. Then, we use the ReliefPlot functionality to generate a relief plot from the array of height values.
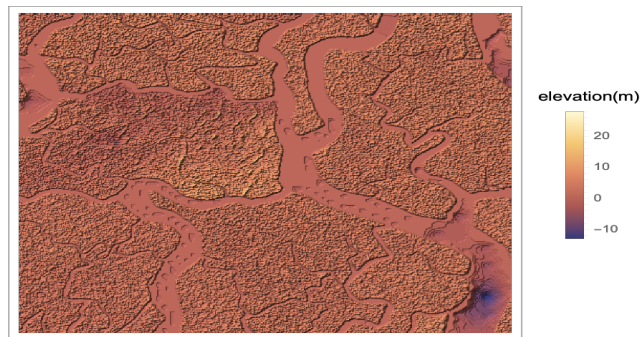
Figure 11 : Relief plot of the Sundarbans National Park

Next, we create an image using the array of geo-elevation values, and use the **ImageAdjust** function - which adjusts the levels in image, rescaling them to account for bad lighting.
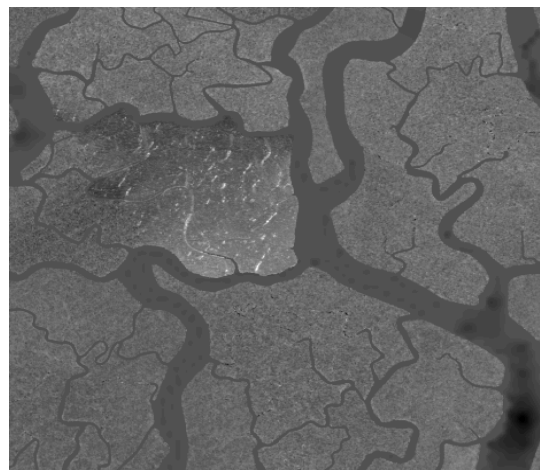
**Figure 12 : Adjusted Binary Image of Sundarbans National Park**

The watershed components functionality returns the transform of an image, computes the watershed transform of *image*, and returns the result as an array in which positive integers label the catchment basins. We then create an image on the basis of the watershed components, and then apply color negate to the image to create a binary image. This allows us to clearly see the de-segmentation of the basis into sub-basins, which is very useful.

12

Figure 13 : Watershed Components of the Sundarbans

Next, we apply functions such as Erosion and Dilation to obtain data about the image, and then create an association thread between the two datasets. We then create a function to evaluate the components of the image that are minimum and at the border of the image, and weed them out. The interaction between various basin components, such as how water flows between them, is known as the hydrological connectedness of a river basin. A graph can be used to illustrate this connectivity, with each vertex representing a section of the basin and the edges denoting the links among them. In this context, clusters are collections of linked vertices that constitute functional units in the hydrographical ecology of the river basin. These groups represent bigger river basins or regions within it that have comparable hydrological properties. It is a simplification approach that makes it simpler to view and evaluate the overall connectivity and relationships to use centroids to represent the positions of vertices. Each sub-basin can be represented by a single point using centroids.
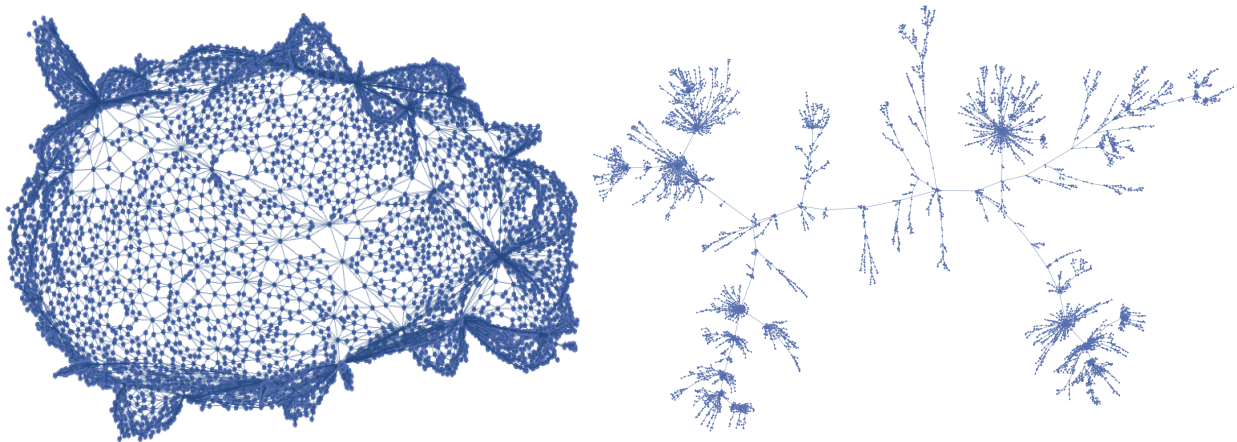
Figure 14: Hydrological Connectedness of River Basins in the Sundarbans and Transitive Reduction Graph

We can also use images, which better represent the structure of the basins to create a more accurate model of water-basin delineation. This image represents another version of the earlier map, there is a lot of segmentation and merging of water basins.

Figure 15: Satellite Imagery of Indian Mangroves

We create a binarized version of the image by using ColorNegate, and weighting the dominant colors in the image, and then use the MorphologicalGraphComponents functionality to perform water-basin delineation. The algorithm for river basin delineation is provided below.

- Invert the colors in the image using the ColorNegate function. Weight the dominant colors in the image.
- Use the MorphologicalGraphComponents functionality to identify connected components in the image.
- Label the connected components as different water basins.

These steps can be used to accurately delineate water basins in images. This can be useful for a variety of purposes, such as hydrological modeling, environmental monitoring, and disaster management.
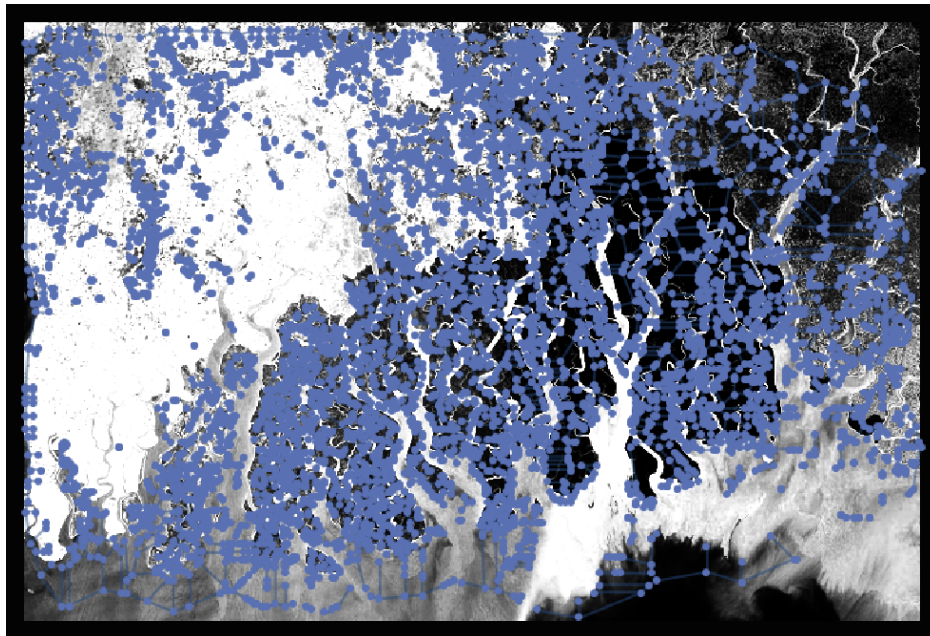
Figure 16 : Water-basin Delineation of Indian mangroves

As we can see, the result isn't particularly impressive and contains a plethora of disconnected vertices - but it still identifies some structures properly. In order to improve upon the previous result, we can create a list of the WeaklyConnected Graph Components of the Morphological Graph, and then iterate over then. We can also set a limit - including non-trivial graphs that have more than 12 vertices in order to get a better result. Furthermore, we

can use the KCoreComponent functionality and highlight the important subgraphs in a complex graph system. These watershed-delineations are way more accurate compared to the first one. Another way to do this is to label the boundary between two adjacent sub-basins by the indexes of corresponding sub-basins and then gauge at how the vertices are connected together and what are the corresponding clusters made out of connected vertices. This would mean that clusters represent larger basins that form a unique hydro-graphical ecosystem with a unique water graph.
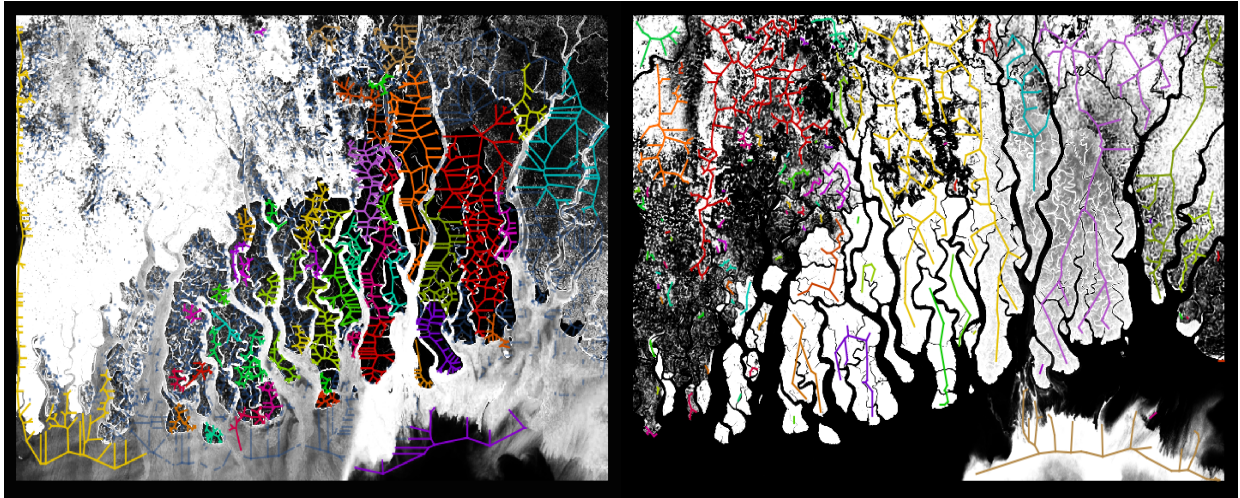
Figure 17: Basin Delineation by Using Sub-Basins as Centroids

3.6 Investigation on Simple River Systems

Simple river systems may present challenges to the floodplain analysis: rural landscapes may erroneously increase the complexity of the mapping process, providing wrong measurements of rainfall and flooding elevation. These problems may cause the prediction to be inaccurate, hence our motivation to apply the code generally to all locations through better cleaning algorithms.

We explore an example in Jackson, Mississippi, using the measurements taken from dominantColorsCity, canonicalColorValueMap, cleanupRules, cityColorCoverage, cityWeightedByColor, permeability, intensity, intensityCalibrated, acres, peakRunoff, totalRiverIncrease. In the jacksonGeo model, we simulated 152.786 feet of heavy rainfall over 200 hours in Jackson, Mississippi. Then, we evaluated the ReliefPlot and ListPlot3D using the peakRunoff data and we were able to determine using the rational method ($Q = CiA$).
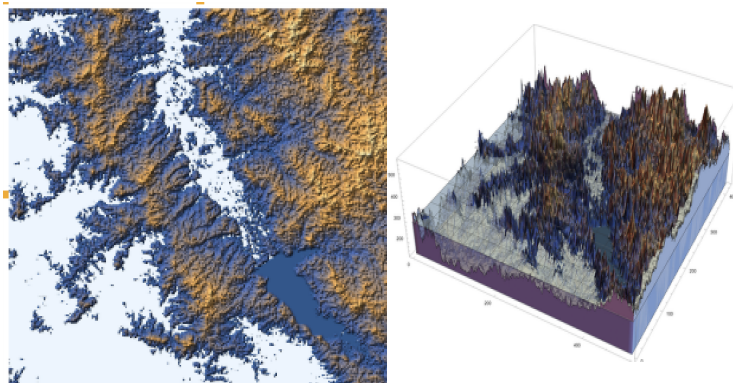

Figure 18 : Relief plot and 3D plot for floods in Jackson,Mississippi

3.7   Investigation on Complex River Systems

Complex river systems may present challenges to the floodplain analysis: urban landscapes have varying ranges of elevation, diverse river tributaries, and sporadic weather. These problems may cause the prediction to be inaccurate, hence our motivation to apply the code generally to all locations through better cleaning algorithms. Note that we added the parameter cityDimensions to make the plot ranging inclusive of all points in the 20 by 20 mile area. We explore an example in Anchorage, Alaska, using the measurements taken from the dominant-ColorsCity, canonicalColorValueMap, cleanupRules, cityColorCoverage, cityWeightedByColor, permeability, intensity, intensityCalibrated, acres, peakRunoff, totalRiverIncrease parameters to pick out the river color, connect them into polygons, and conduct the $Q = CiA$ framework to represent the river increase. In the anchorageGeo model, we simulated 1527.86 feet of heavy rainfall over 2000 hours in Anchorage, Alaska. Then, we evaluated the ReliefPlot and ListPlot3D using the peakRunoff data we were able to determine using the rational method ($Q = CiA$). .

Here are Jackson's relief and 3D plots, using the variables anchorageData, levelPlot, reliefMap, cityDimensions, and floodPlot:
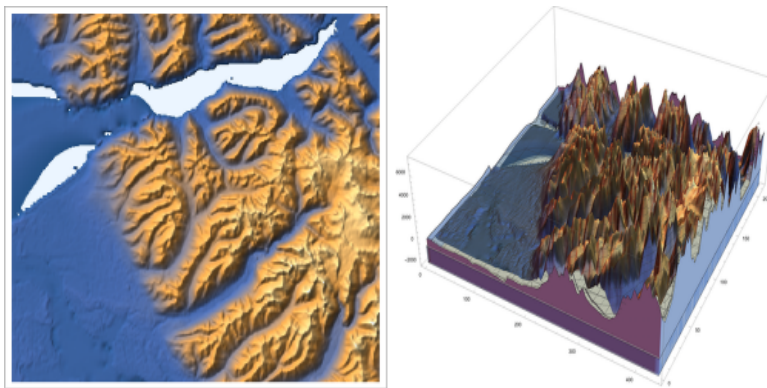

Figure 19: Construction of relief plot and 3D plot for floods in Anchorage, Alaska
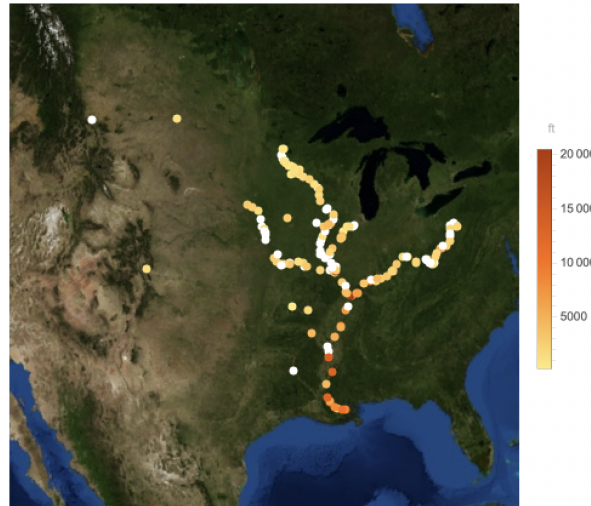
3.8   Analysis of Stream Width

We can model the river width of a certain river and its contributing tributaries through determining the length of notable bridges that cross the river from its origin to its delta. Specifically, we will use the functions FilteredEntityClass and GeoRegionValuePlot to create our river width weights.

Here is an example from the Missouri River:
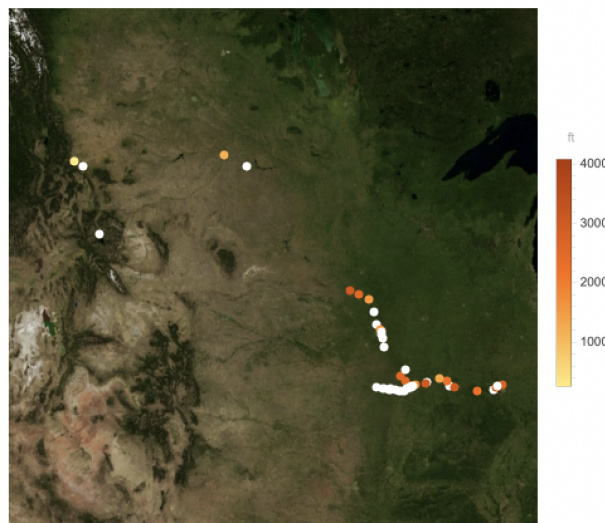
Figure 20 : Stream width of the Missouri River

A more comprehensive example that incorporates the river delta in relation with the origin is the Mississippi River Here, we can see the gradual increase of river width as it moves towards the river delta:


Figure 21 : Stream width of the Mississippi River

3.9 Statistical Analysis of Annual Peak Flow Data

We consider the case of 101 years of annual peak flow data (in cf/s, or cubic feet per second) for the Rio Grande at Embudo, New Mexico.The length of the Rio Grande is 1,896 miles (3,051 km), making it the 4th longest river in North America by main stem.

It originates in south-central Colorado, in the United States, and flows to the Gulf of Mexico.The Rio Grande drainage basin (watershed) has an area of 182,200 square miles (472,000 km^2); however, the endorheic basins that are adjacent to and within the greater drainage basin of the Rio Grande increase the total drainage-basin area to 336,000 square miles (870,000 km^2). According to the US Government, the continuous geomorphologic changes in the Middle Rio Grande in New Mexico have been of interest for many governmental agencies (USDA). This makes studying the Rio Grande extremely interesting.
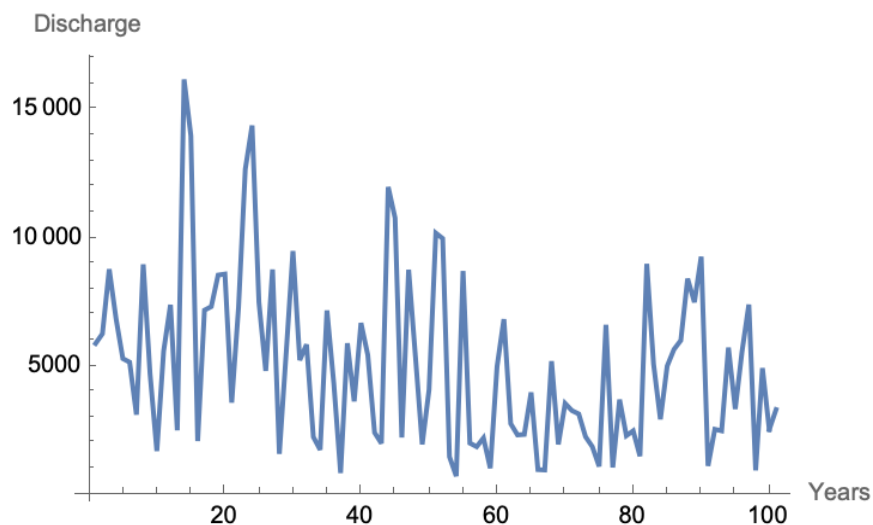
Figure 22 : 101 years of annual peak flow data for the Rio Grande river
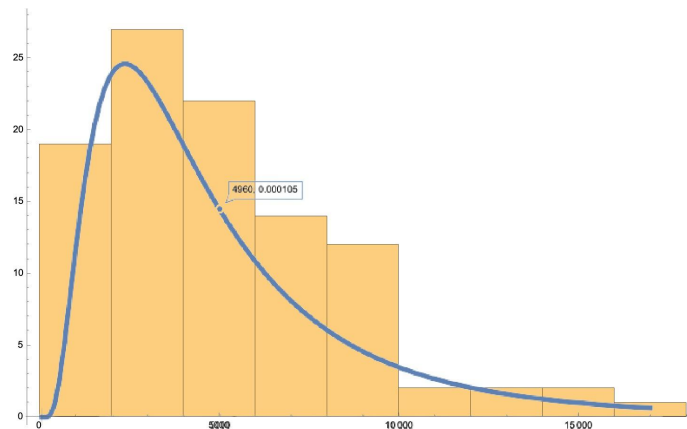
3.10 Probability Density Functions

We plot the values on a histogram and notice that the data is very skewed towards the right. Applying the logarithmic function to each value makes the table more balanced.
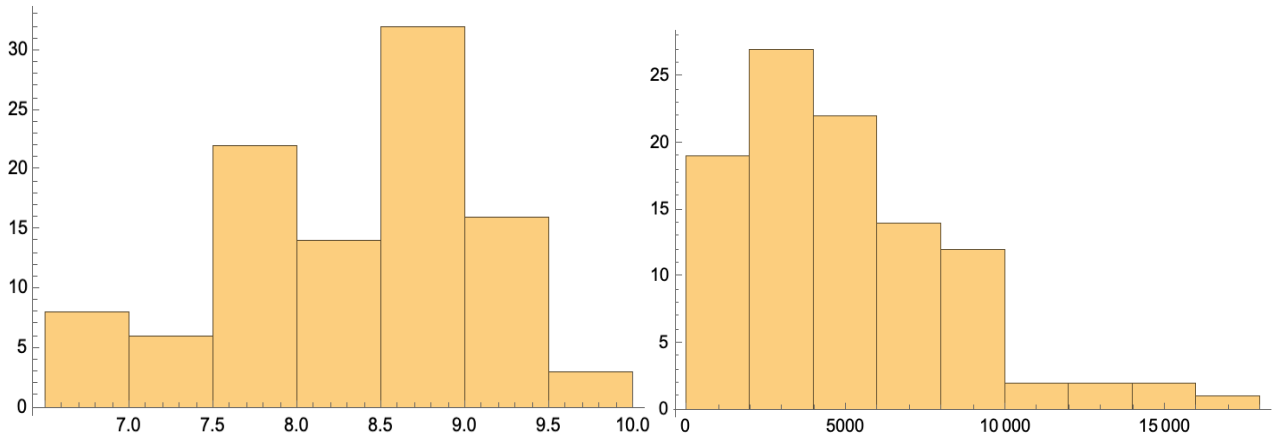
Figure 23 : Histogram Data after and before logarithmic correction on Rio Grande

Now, we can find the mean values of the logarithm of the peak-flow values and their standard deviation and create a **Probability Density Function (PDF)** using the LogNormalDistribution functionality - in which the maximum entropy probability distribution for the random variate is measured. This is then overlaid on top of the histogram:
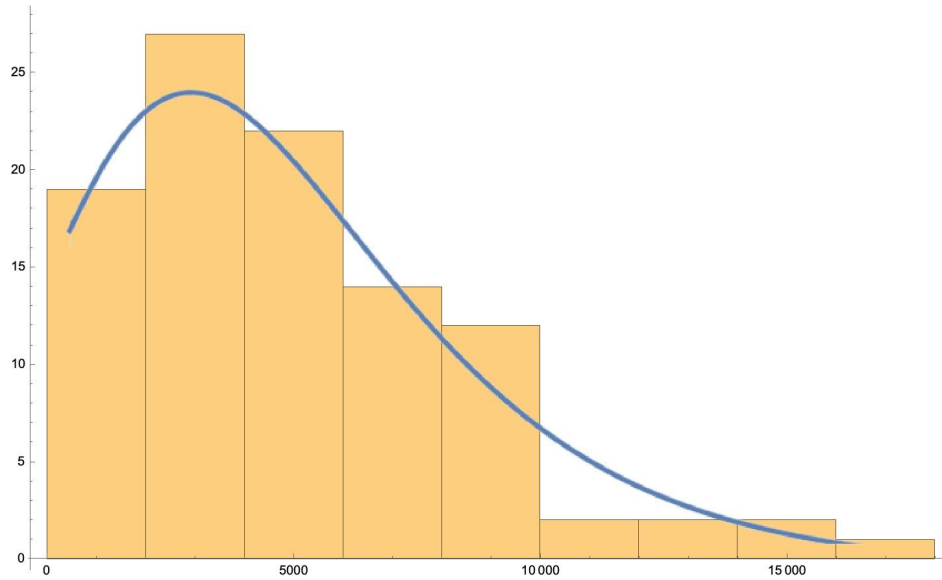

Figure 24 : Correlation between the PDF and Histogram

We can see a correlation between the histogram and the probability density function, but it can be improved. Therefore, in order to improve it, we move towards another PDF. We use ExtremeValueDistribution, which is an important tool in statistical analysis. Analogous to the emergence of normal and stable distributions as natural limit distributions when dealing with linear combinations, such as means of independent variables, ExtremeValueDistribution arises as an inherent limit distribution when examining the minimum and maximum operations of independent variables.

$\beta = StandardDeviation[PeakFlow] \times Sqrt[6] \div 3.141592 = 2599.56$

$\alpha = Mean[PeakFlow] - 0.5772$

We overlay it on top of the data and see a more positive correlation.

18

Figure 25: Correlation between Extreme Value Distribution PDF and Histogram

3.11 Using Cumulative Distribution Functions

Next, we can look at a Cumulative Distribution Function (ExtremeValueDistribution). It is obtained by summing up the probability density function and getting the cumulative probability for a random variablusing the values of alpha and beta.
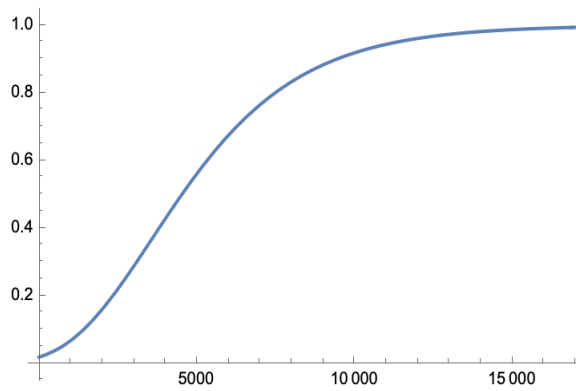
Figure 26 : Cumulative Distribution Function using ExtremeValueDistribution

We also look at another **CDF**, this time - it's the **LogNormalDistribution** function which uses the mean values and the standard deviation
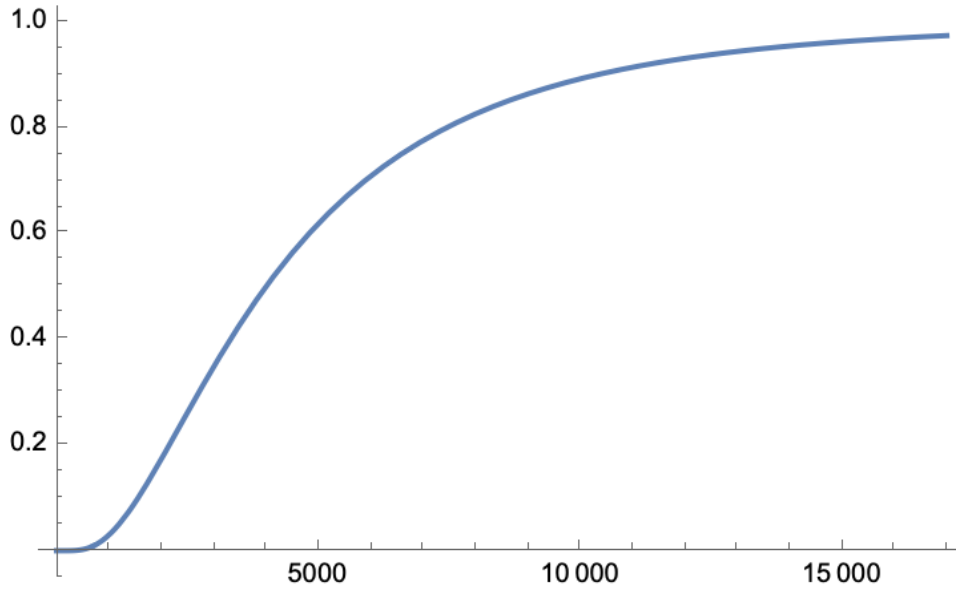
Figure 27 : Cumulative Discrete Function using Log Normal Distribution

And finally, we can show the intersection of the two cumulative discrete functions
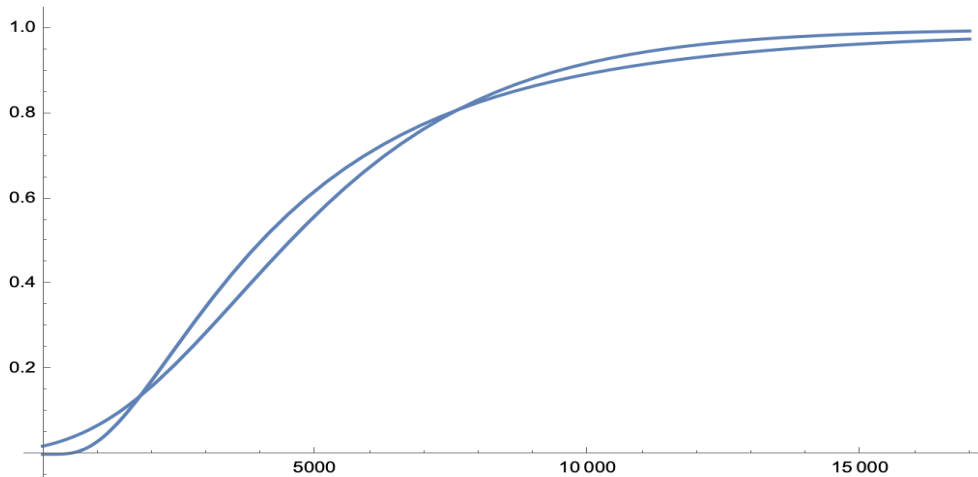
Figure 28 : Comparison Between Cumulative and Log Normal Distributions

3.12   Kumaraswamy Distribution

We can also perform statistical analysis for lakes and other small water bodies. We take the example data of Lake Mead's water levels, and then calculate the Kumaraswamy-Distribution for it.

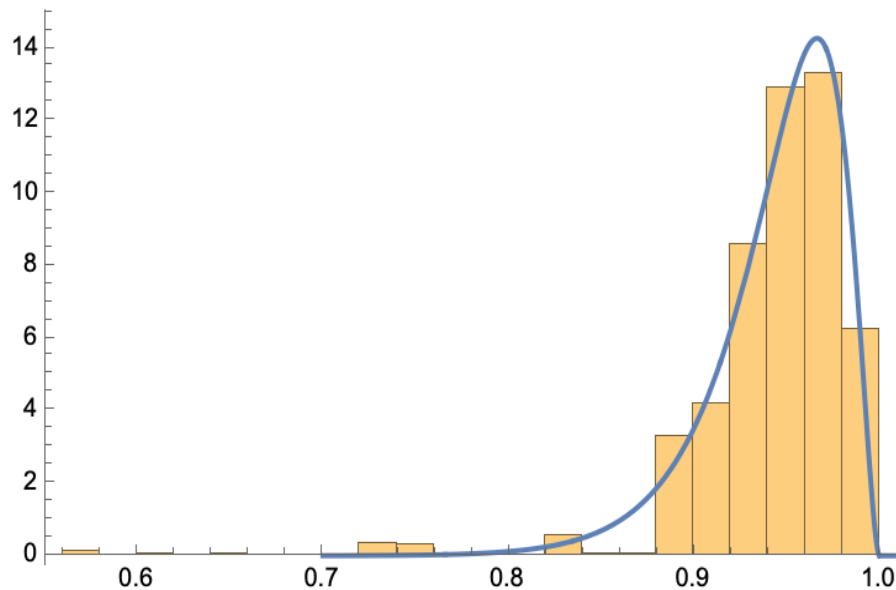**Figure 29: Kuramaswamy distribution function overlaid on top of Histogram for Lake Mead**

4 Discussion

4.1 Visualization of Elevation Data

GeoElevationData proves to be a comprehensive resource, allowing access to precise elevation information for any geographic location. By default, it returns orthometric height, which is considered the most reliable tool for measuring height with respect to mean sea level. However, alternative heights, such as geodetic height and undulation height, can also be obtained by varying parameters, enhancing the flexibility of elevation visualization. The ReliefPlot function in the Wolfram Language serves as a powerful tool for generating relief maps from height values obtained through GeoElevationData. Relief maps are essential for facilitating the visual recognition of terrain features, providing researchers and cartographers with a detailed representation of the terrain's characteristics. Overall, the combination of GeoElevationData and ReliefPlot in the Wolfram Language enables precise visualization and analysis of elevation data, finding applications in cartography, geography, environmental science, and various other domains.

4.2 Relief Maps and Floodplain Analysis

Watergate provides a novel approach for identifying rivers and tributaries in GeoLocations using the Wolfram Language. The authors point out the limitations of current methods for analyzing river tributaries in the Wolfram Language, which are primarily limited to "notable" rivers and streams due to the representation of rivers as Entities rather than GeoEntities. Consequently, the database lacks information on tributary points, connectedness, and stream order identification. To address this limitation, the authors present a step-by-step methodology to find rivers and tributaries, employing image processing and mathematical morphology techniques. The approach begins by taking the example of Paris and the river Marne, acting as a tributary to the river Seine. Utilizing the VectorMinimal parameter, the authors convert individual components on the map into manipulable polygons, facilitating the visualization of rivers. By identifying water primitives through their light-blue color, they extract water-related graphics from the map.

However, certain properties in the MorphologicalGraph are not suitable for rivers with large bodies of water, as it fails to depict tributaries accurately and assess the distance between them. To overcome this limitation and create an acyclic representation, the authors employ the TransitiveReductionGraph function. This function reduces the graph to have the same vertices but with fewer edges, making it acyclic and devoid of loops. Converting the acyclic morphological graph to a tree allows the authors to gauge the structural information of the river, particularly when it splits. By applying MorphologicalBranchPoints, the authors identify stream splits and implement cleaning mechanisms to remove extraneous water sources, restoring the river to its original size.

The proposed approach showcases the potential of the Wolfram Language in identifying rivers and tributaries, even in locations where traditional river data extraction methods fall short. The combination of image processing and mathematical morphology enables the creation of a more accurate and comprehensive representation of river systems, facilitating a deeper understanding of their connectivity and structure. The approach holds promise for applications in hydrology, cartography, and environmental studies, enabling researchers to analyze river networks and their tributaries with greater precision.

4.3 Horton-Strahler Stream Order

The Horton-Strahler stream order is numerical measure of the branching complexity of a river. The algorithm, first developed by Robert E. Horton and Arthur Newell Strahler, assigns a Strahler number to each node in a tree-like structure representing the river network. The process of assigning the Strahler number to a leaf in the tree involves three rules: if the node is a leaf, its Strahler number is one; if the node has one child with Strahler number i and all other children have Strahler numbers less than i, the Strahler number of the node is i; and if the node has two or more children with Strahler number i and no children with a greater number, the Strahler number of the node is i + 1.

The paper also introduces the concept of the Bifurcation ratio, which is an accompanying ratio to the Horton-Strahler algorithm. The nth Bifurcation Ratio is defined as the ratio of the number of vertices of order i to the number of vertices of order (i+1). The overall bifurcation ratio, in this case, is calculated by taking the average of all the bifurcation ratios of order i, yielding a value of 1.57692. The implementation of the Horton-Strahler algorithm and the calculation of the bifurcation ratio in the Wolfram Language demonstrate the language's effectiveness in handling complex tree-like structures and performing numerical calculations. This algorithm and ratio offer valuable insights into the branching patterns of river networks, aiding hydrologists, geographers, and environmental scientists in understanding the flow and connectivity of river systems. The simplicity and computational efficiency of the implementation make it a useful tool for analyzing river networks and studying their hydrological properties. The Horton-Strahler algorithm and the bifurcation ratio contribute to a better understanding of river morphology, and their integration into the Wolfram Language expands its utility in hydrological analysis and research.

4.4 Watershed Delineation

Watergate focuses on implementing the rational method, a widely used approach for determining peak discharges in stormwater management. Traditionally applied to size storm sewers, channels, and other stormwater structures, the rational method utilizes the formula $Q = CiA$, where Q represents the peak rate of runoff, C is the runoff coefficient, i denotes the average intensity of rainfall, and A represents the watershed area. The authors demonstrate how the Wolfram Language can be employed to calculate each variable of the rational method and parameterize them for any geographic location. They start by finding the runoff coefficient, which is determined by associating colors in a map with weights. By using Nearest and ReplaceAll, the closest colors are matched with the corresponding weights. The DominantColors function aids in determining color coverage in different regions of the map through k-means clustering, ultimately leading to the calculation of the runoff coefficient.

For a practical application of the rational method, the authors calculate the data for the city of Juneau, Alaska, including peak runoff, permeability, intensity calibrated, and the area in acres. A river runoff model is then created by multiplying the calculated peak runoff (Q) by the inverse of rainwater flowing into the river basin. This model represents the increase factor of the river over time due to rainwater.The implementation of the rational method in the Wolfram Language showcases the language's capabilities in numerical calculations, data analysis, and spatial modeling. By providing tools for accessing weather data, processing geospatial information, and performing calculations, the Wolfram Language streamlines the process of analyzing stormwater runoff and determining peak discharges. The practical application of the rational method in the context of the Juneau river runoff model further demonstrates the utility of the Wolfram Language in hydrological modeling and floodplain analysis.

4.5 Simple and Complex River Systems

Simple river systems, often found in rural landscapes, may lead to inaccuracies in the mapping process, resulting in erroneous measurements of rainfall and flooding elevation. To overcome these limitations and ensure general applicability, the authors propose the use of better cleaning algorithms. An example in Jackson, Mississippi, is explored to demonstrate the application of the proposed methodology. The authors utilize various measurements, such as dominantColorsCity, canonicalColorValueMap, cleanupRules, cityColorCoverage, cityWeightedByColor, permeability, intensity, intensityCalibrated, acres, peakRunoff, and totalRiverIncrease. They create the jacksonGeo model, simulating heavy rainfall of 152.786 feet over 200 hours in Jackson. The ReliefPlot and ListPlot3D are

then evaluated using peakRunoff data, and the rational method ($Q = CiA$) is employed to determine floodplain conditions. Complex river systems, typically found in urban landscapes, present additional challenges due to their varying elevation ranges, diverse river tributaries, and sporadic weather patterns. To address these complexities, the authors again emphasize the application of their code with better cleaning algorithms for general use. The parameter cityDimensions is introduced to ensure inclusivity of all points within a 20 by 20 mile area. An example in Anchorage, Alaska, is used to illustrate the effectiveness of the proposed approach in handling complex river systems. Measurements such as dominantColorsCity, canonicalColorValueMap, cleanupRules, cityColorCoverage, cityWeightedByColor, permeability, intensity, intensityCalibrated, acres, peakRunoff, and totalRiverIncrease are considered in the anchorageGeo model. Heavy rainfall of 1527.86 feet over 2000 hours is simulated in Anchorage, and the ReliefPlot and ListPlot3D are evaluated using peakRunoff data through the rational method.

The relief and 3D plots of Jackson and Anchorage showcase the utility of the proposed methodology in floodplain analysis. By leveraging the variables anchorageData, levelPlot, reliefMap, cityDimensions, and floodPlot, the authors demonstrate the capability of the Wolfram Language to handle geospatial data, perform flood modeling, and visualize complex river systems.

4.6 Statistical Analysis

Watergate first focuses on a comprehensive statistical analysis of 101 years of annual peak flow data for the Rio Grande at Embudo, New Mexico, measured in cubic feet per second (cf/s). The initial step involves plotting the data on a histogram, revealing a right-skewed distribution. To address this skewness, the Log function is applied to each value, resulting in a more balanced dataset.

To enhance the correlation, the ExtremeValueDistribution is employed for the next PDF. The ExtremeValueDistribution is suitable for modeling minimum and maximum operations of independent variables, making it a natural choice for analyzing extreme values in peak-flow data. By adjusting the parameters alpha and beta, the PDF is optimized and overlaid on the data, revealing a more positive correlation. The analysis delves into Cumulative Distribution Functions (CDF) to gain deeper insights into the data. The CDF for ExtremeValueDistribution is computed using the values of alpha and beta, providing valuable information about the distribution of extreme values in the dataset. Additionally, the CDF for LogNormalDistribution is also evaluated using mean values and standard deviation. Watergate then expands its scope to examine Lake Mead's water levels, using cumulative discrete functions to model the data. The Kumaraswamy-Distribution is calculated for the data, allowing researchers to estimate the probability of drought occurrences in the region. This analysis is visualized, and a Probability Distribution Function is created for the Estimated Kumaraswamy Distribution, providing further insights into the probability of droughts in the area.

The research paper showcases a comprehensive statistical analysis of annual peak flow data, employing a range of probability distributions and cumulative distribution functions. By utilizing the Wolfram Language's powerful statistical functionalities, the study provides valuable insights into the hydrological behavior of the Rio Grande at Embudo, New Mexico, and its implications for water resource management and flood risk assessment. This research contributes to the field of hydrology and statistical analysis, offering a robust framework for analyzing extreme values in hydrological data and aiding in decision-making processes for water management strategies.

5 Conclusion and Future Directions

In our project, we first established the elementary framework for detecting river tributaries based on geographic location, establishing nodes for river tributary branches, and creating trees for river tributaries. Secondly, we created the frameworks for floodplain analysis through geographic elevation data and applied the rational method framework ($Q = CiA$). Further, we analyzed population density and created functions to generalize for all geographic locations. Finally, we combined our 2 findings to create a comprehensive 3D model that models both river tributary splits and flood plains.

In the future, we would like to pursue a more in-depth examination of river tributaries: river turbidity, river velocity, and water elevation level. We would also like to create a more accurate representation of overflowing rivers rather using differential equations rather than a simple linear function. Once the incorporation of river tributaries as GeoEntities is implemented, we hope to update our model with more accurate and relevant data, otherwise, we hope to continue to work on additional features and develop an application for ease of access.

6 Acknowledgment

References

[1] United Nations. *Global Issues - Water*. UN News Center, 2020.

[2] Christopher B. Field et al., editors. *Managing the Risks of Extreme Events and Disasters to Advance Climate Change Adaptation: Special Report of the Intergovernmental Panel on Climate Change*. Cambridge University Press, 2012.

[3] Kevin E. Trenberth. *Conceptual Framework for Changes of Extremes of the Hydrological Cycle with Climate Change*. Climatic Change, 42(1):327–339, 1999.

[4] Yukiko Hirabayashi et al. *Global Flood Risk Under Climate Change*. Nature Climate Change, 3(9):816–821, 2013.

[5] *Cyclone Idai Situation Report*, 2019.

[6] Abhas K. Jha, Robin Bloch, and Jessica Lamond. *Cities and Flooding: A Guide to Integrated Urban Flood Risk Management for the 21st Century*. The World Bank, 2012.

[7] Emergency Relief Coordination Center. *Thailand: Floods*. Technical report, 2011.

[8] John M. Barry. *Rising Tide: The Great Mississippi Flood of 1927 and How It Changed America*. Simon and Schuster, 1998.

[9] Sharon T. Ashley and Walker S. Ashley. Flood fatalities in the united states. *Journal of Applied Meteorology and Climatology*, 47(3):805 – 818, 2008.

[10] Keith Beven and Jim Freer. *Equifinality, Data Assimilation, and Uncertainty Estimation in Mechanistic Modelling of Complex Environmental Systems Using the GLUE Methodology*. Journal of Hydrology, 249(1-4):11–29, 2001.

[11] Michael B Abbott, James C Bathurst, Jean A Cunge, Patrick E O'Connell, and Jorn Rasmussen. An introduction to the european hydrological system—systeme hydrologique europeen,"she", 1: History and philosophy of a physically-based, distributed modelling system. *Journal of hydrology*, 87(1-2):45–59, 1986.

[12] Ezio Todini. *The ARNO Rainfall–Runoff Model*. Journal of Hydrology, 175(1-4):339–382, 1996.

[13] John A. Cunge. *On the Subject of a Flood Propagation Computation Method (Muskingum Method)*. Journal of Hydraulic Research, 7(2):205–230, 1969.

[14] David R. Maidment. *GIS and Hydrological Modelling*. Progress in Physical Geography, 23(2):269–281, 1999.

[15] Ven Te Chow, David R. Maidment, and Larry W. Mays. *Applied Hydrology*. McGraw-Hill, 1988.

[16] Kuo-lin Hsu et al. *Self-Organizing Linear Output Map (SOLO): An Artificial Neural Network Suitable for Hydrologic Modeling and Analysis*. Water Resources Research, 38(12):38–1, 2002.

[17] Stephen Wolfram. *The Design of a New Kind of Science*. The Mathematica Journal, 9(3), 2005.

[18] Bob Carpenter. *Artificial Intelligence and the Wolfram Language*. Wolfram Blog, 2018.

[19] Roman E. Maeder. *Programming in Mathematica*. Addison-Wesley, 1991.

[20] David B. Wagner. *Powerful Ideas in the Classroom: Using Squeak to Enhance Math and Science Learning*. The Journal of Computers in Mathematics and Science Teaching, 20(1):7–28, 2001.

[21] Wolfram Research. *Geography & Maps*. Wolfram Language & System Documentation Center, `https://reference.wolfram.com/language/guide/GeographyAndMaps.html`, 2023.

[22] Hannah L. Cloke and Florian Pappenberger. *Ensemble Flood Forecasting: A Review*. Journal of Hydrology, 375(3-4):613–626, 2009.

[23] Tamlin M. Pavelsky and Laurence C. Smith. *RivWidth: A Software Tool for the Calculation of River Widths from Remotely Sensed Imagery*. IEEE Geoscience and Remote Sensing Letters, 5(1):70–73, 2008.

[24] David G. Tarboton. *A New Method for the Determination of Flow Directions and Contributing Areas in Grid Digital Elevation Models*. Water Resources Research, 33(2):309–319, 1997.

[25] Peter Vogt et al. *Analyzing the Impact of Grid Resolution in Large-Scale Hydrological Modelling by use of GIS*. Hydrological Processes, 11(7):779–795, 1997.

[26] Richard H. McCuen. *Hydrologic Analysis and Design*. Pearson, 2004.

[27] Warren Viessman Jr. and Gary Lewis. *Introduction to Hydrology*. Pearson; 5th edition, 2002.

[28] Martin Ester et al. *A Density-Based Algorithm for Discovering Clusters in Large Spatial Databases with Noise*. In *KDD-96 Proceedings*, pages 226–231, 1996.

[29] Robert E Horton. Erosional Development of Streams and Their Drainage Basins; Hydrophysical Approach to Quantitative Morphology. *GSA Bulletin*, 56(3):275–370, 03 1945.

[30] Arthur N Strahler. Hypsometric (Area-Altitude) Analysis of Erosional Topography. *GSA Bulletin*, 63(11):1117–1142, 11 1952.

[31] Arthur N Strahler. Quantitative analysis of watershed geomorphology. *Eos, Transactions American Geophysical Union*, 38(6):913–920, 1957.

A Appendix A

The github repository which includes all of the code can be found at:

`https://github.com/navvye/WaterGate`